

Systems Science & Control Engineering

An Open Access Journal

ISSN: (Print) (Online) Journal homepage: www.tandfonline.com/journals/tssc20

Implementation of sensorless contact force estimation in collaborative robot based on adaptive third-order sliding mode observer

Quang Dan Le & Hee-Jun Kang

To cite this article: Quang Dan Le & Hee-Jun Kang (2022) Implementation of sensorless contact force estimation in collaborative robot based on adaptive third-order sliding mode observer, Systems Science & Control Engineering, 10:1, 507-516, DOI: [10.1080/21642583.2022.2063201](https://doi.org/10.1080/21642583.2022.2063201)

To link to this article: <https://doi.org/10.1080/21642583.2022.2063201>



© 2022 The Author(s). Published by Informa UK Limited, trading as Taylor & Francis Group.



Published online: 10 May 2022.



Submit your article to this journal [↗](#)



Article views: 1106



View related articles [↗](#)



View Crossmark data [↗](#)



Citing articles: 3 View citing articles [↗](#)

Implementation of sensorless contact force estimation in collaborative robot based on adaptive third-order sliding mode observer

Quang Dan Le and Hee-Jun Kang

Department of Electrical, Electronic and Computer Engineering, University of Ulsan, Ulsan, South Korea

ABSTRACT

In this paper, we propose the estimation of contact force in a collaborative robot without explicit force-sensing based on the adaptive third-order sliding mode observer. An adaptive third-order sliding mode observer was designed to estimate the contact force based only on the position measurement. The information from the observer was used for admittance control and emergent stop control when the robot interacts with a human. The experimental results with the emergent stop control and admittance control, using the proposed contact force estimation for the 3-DOF AT2-FARA robot manipulator, illustrate the capability of the proposed system in real-world application.

ARTICLE HISTORY

Received 13 December 2021
Accepted 4 April 2022

KEYWORDS


Physical human-robot interaction; sliding mode observer; third-order sliding mode observer; admittance control sensorless; collaborative robot

1. Introduction

Nowadays, with the development of hardware technology and software, robots are becoming more and more common and friendly to humans. In the past, most robots only worked in industrial environments and in a separate space from human work areas to ensure worker safety. Moreover, robots are not able to adapt when the environment changes slightly. However, nowadays, robots are friendly and can share the workspace with humans to perform complex tasks. This concept is called collaborative robot (Peshkin et al., 2001) (cobot). In the collaborative solution, thanks to the combination of the precision of robots and the flexibility of humans, robots can work with humans to complete complex tasks. Shortly, robots and humans can assemble household items in daily life (Mörtl et al., 2012). In industry, robots and workers can install equipment for vehicles on the production line (Wojtara et al., 2009). Robots can work with doctors to operate on patients or nurses to care for patients. Cobots can be divided into 5 levels of the combination of humans and robots (Bauer et al., 2016), as in Figure 1. Here, Level 1 is called cell: the traditional operation with the separation of the workspace of robots and workers. Level 2, Coexistence: robots and humans work on the same task, but do not share a workspace. Level 3, Synchronized: While working, the robot and the human share the workspace, but only the robot or the human interacts in the co-working space. Level 4, Cooperation: both can interact in the same

workspace, but do not work on the same product or component. Level 5, Collaboration: humans and robots work in the same workspace on the same product or component simultaneously. It can be seen that from level 3, humans and robots work in the same workspace, so the physical human-robot interaction (pHRI) problem is the background of the cobot. In this matching process, the safety and adaptation of the robot are extremely important because the actions of humans are unpredictable. Therefore, pHRI is a topic of interest to many researchers in the cobot problem.

To implement pHRI, an impedance/admittance controller is often used (Hogan, 1984). The impedance controller computes the force to be applied to the robot's motion, while the admittance controller adjusts the trajectory according to the force on the robot. In general, admittance control is more natural when used in pHRI. To perform admittance controllers or force controllers, force sensors are mounted on the end-effector of a robot or at the actuator in the industry to compute the interaction force of the robot with the environment and humans. For example, most commercial collaborative robots have torque sensors on the actuators, used in admittance controllers. However, this solution significantly increases the cost of the robot. In some cases, such as impedance or hybrid position/force control, the force sensor is attached to the end-effector to measure the force of interaction with the environment (Ferretti et al., 1997). In addition,

CONTACT Hee-Jun Kang  hjkang@ulsan.ac.kr

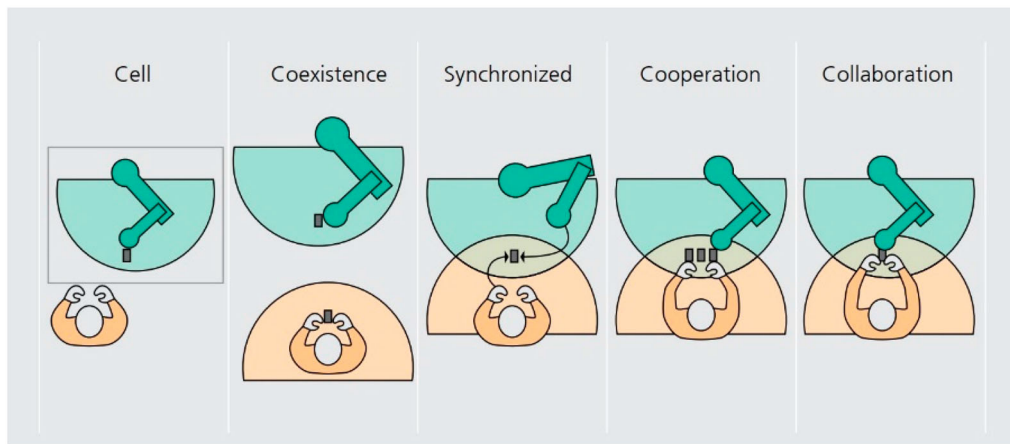


Figure 1. Levels of cooperation between a human and a robot (Bauer et al., 2016).

the optimization and intelligent methods (Chen et al., 2005; Du et al., 2006; Du et al., 2007; Han et al., 2008, 2010; Han & Huang, 2008; Huang, 1999; Huang & Du, 2008; Wang et al., 2010; Wang & Huang, 2009) were used in (Dao et al., 2021; Yu & Perrusquia, 2022) to improve the accuracy of force control. Attaching more devices to the end-effector of the robot can reduce its load capacity and increase its cost. In addition, the force sensor is very sensitive to environmental conditions such as temperature and humidity. Therefore, adding sensors as the solution must be considered to balance efficiency and financial benefits. To solve the economic problem in the force control, many force controls without force sensors have been proposed. For example, in (Geravand et al., 2013; Suita et al., 1995; Wahrburg et al., 2017), the authors directly used current to detect collisions between robots and humans in an immediate stop to ensure safety and application admittance control to the robot controller collaboration. Meanwhile, feedforward torque dithering is proposed by (Stolt et al., 2015) to reduce uncertainty factors due to the accuracy in estimating the force impact when the robot is not moving. In working in the general environment of the cobot, humans and robots may contact at various locations of the robot, so the robot must be able to detect the forces of interaction on the whole body of the robot. This problem is also of interest to many researchers who use a skin for the robot to locate the collision throughout the robot's body, as in (Cirillo et al., 2016; Duchaine et al., 2009). Other authors use stereo cameras (Ebert & Henrich, 2002; Magrini et al., 2014) to detect collisions across the robot and measure the force of the interaction is also a solution that provides high accuracy in the cobot. However, as mentioned earlier, adding external sensors can significantly increase the cost of the robot. Therefore, force control in robots without external sensors is considered a more economical solution

and has attracted the attention of many researchers in recent years. In the methods without the additional external sensors, disturbances observer-based is often used to estimate the contact force of the robot manipulator (Eom et al., 1998; Gaz et al., 2018; Magrini et al., 2015). This observer treats an external force as uncertainties/disturbances and requires an accelerated measurement (Eom et al., 1998). However, in practice, the acceleration measurement is uncommon, and the measured value is often strongly affected by noise. Therefore, (Chen et al., 2018; De Luca & Mattone, 2005; Gaz et al., 2018; Magrini et al., 2015) proposed the disturbances observer to estimate the force of interaction without the measurement of acceleration. In addition, the extended state observer is also used to estimate the force (Hu & Xiong, 2018; Khalil, 2017). The topic of the sliding mode observer is of great interest to many researchers because it can converge in finite time (Fridman et al., 2008; Kommuri et al., 2018). Moreover, the controller based on the sliding mode method is effective in low-level control (Jung et al., 2004; Le & Kang, 2020; Van et al., 2017). Most sliding mode observers usually require only position measurement, which is very convenient to apply in real systems. The two major drawbacks of the sliding mode are the proof of stability and the choice of coefficient, which depends on the information about the upper bound of disturbances. Fortunately, (Cruz-Zavala & Moreno, 2016; Ortiz-Ricardez et al., 2015) proved a method to demonstrate the stability of the high-order sliding mode observer. And in (Bahrami et al., 2018; Luo et al., 2018), the solution uses the adaptive coefficients method to ignore the information about the upper bound of the perturbations.

This article extends the article (Le & Kang, 2021) in which an adaptive third-order sliding mode observer is proposed for estimating the contact force in pHRI for cobot. The information of the estimated force will be used

directly in the immediate robot stop or for admittance control in pHRI. The proposed results on 3-DOF robot manipulator are presented to confirm the effectiveness of the proposal in a real robot system.

The main contributions of this work are briefly listed:

- (1) The proposed method can estimate the contact force in physical human-robot interaction without a force sensor. This can significantly reduce the price of collaborative robots.
- (2) The contact force estimation only requires position measurement and is easily applicable in a real robot system.
- (3) Experimental results illustrate the capability of the proposed method in a real-world application.

The rest of this article is presented as follows. In Section 2, the dynamics of the robot manipulator is presented. Section 3, an adaptive third-order sliding mode observer is proposed to estimate the contact force in pHRI. In Section 4, the experimental results of the proposed on 3-DOF robot manipulator with robot stop and admittance control for pHRI are presented. Finally, the conclusions and future work are given in Section 5.

2. Dynamics model of robot manipulator

The dynamics model of a robot manipulator for n-degree in contact with a human is given as

$$M(q)\ddot{q} + C(q, \dot{q})\dot{q} + G(q) = \tau + \tau_{\text{int}}, \quad (1)$$

where $\ddot{q}, \dot{q}, q \in \mathbb{R}^n$ are the vectors of joint accelerations, velocity and position, respectively. $M(q) \in \mathbb{R}^{n \times n}$ is the inertia matrix, $C(q, \dot{q}) \in \mathbb{R}^n$ represents the centripetal and Coriolis matrix, $G(q) \in \mathbb{R}^n$ represents the gravitation torques. τ is torque provided at joint. τ_{int} is the interaction force.

Property 1: The matrix $\dot{M}(q) - 2C(q, \dot{q})$ is skew-symmetric.

Property 2: $\|M^{-1}(q)\| < \alpha$ where α is a positive constant.

3. Contact force estimation

In this section, the estimation of the contact force based on an adaptive third-order sliding mode observer is proposed.

The dynamic model (1) can be rewritten in state space as

$$\begin{cases} \dot{x}_1 = x_2 \\ \dot{x}_2 = f(x_1, x_2, u) + \phi(x_1, x_2, t) \end{cases} \quad (2)$$

where $x_1 = q$, $x_2 = \dot{q}$, $u = \tau$, $f(x_1, x_2, u) = M^{-1}(q)(\tau - C(q, \dot{q}) - G(q))$ and $\phi(x_1, x_2, t) = M^{-1}(q)(\tau_{\text{int}})$.

An adaptive third-order sliding mode observer is designed as

$$\begin{cases} \dot{\hat{x}}_1 = \kappa_1 |e_1|^{\frac{2}{3}} \text{sgn}(e_1) + \hat{x}_2 \\ \dot{\hat{x}}_2 = \kappa_2 |e_1|^{\frac{1}{3}} \text{sgn}(e_1) + f(x_1, \hat{x}_2, u) + \hat{x}_3 \\ \dot{\hat{x}}_3 = \kappa_3 \text{sgn}(e_1) \end{cases} \quad (3)$$

where \hat{x}_1 and \hat{x}_2 are estimations of x_1 and x_2 , respectively. $e_1 = x_1 - \hat{x}_1$, \hat{x}_3 is the estimation of $\phi(x_1, x_2, t)$. Let $L = \kappa_3, \kappa_2 = 5.3L^{\frac{2}{3}}$ and $\kappa_1 = 3.34L^{\frac{1}{3}}$ and the update law:

$$\dot{L} = \begin{cases} \bar{L}|e_1| \text{sign}(|e_1| - \varepsilon) & \text{if } L > \lambda \\ 0 & \text{if } L \leq \lambda \end{cases} \quad (4)$$

Lemma 3.1: Let $\eta : \mathbb{R}^n \rightarrow \mathbb{R}$ and $\gamma : \mathbb{R}^n \rightarrow \mathbb{R}_+$, that is $\gamma(x) \geq 0 \forall x$, be two continuous homogeneous functions, with weights $r = (r_1, \dots, r_n)$ and degrees m , such that $\{x \in \mathbb{R}^n \setminus \{0\} : \gamma(x) = 0\} \subseteq \{x \in \mathbb{R}^n \setminus \{0\} : \eta(x) < 0\}$. Then, there exists a real number λ^* such that, for all $\lambda \geq \lambda^*$ for all $x \in \mathbb{R}^n \setminus \{0\}$, and some $c > 0$, $\eta(x) - \lambda\gamma(x) < -c\|x\|_{r,p}^m$.

Lemma 3.2: (Young's inequality): For any positive real numbers $a > 0$, $b > 0$, $c > 0$, $p > 1$ and $q > 1$ with $\frac{1}{p} + \frac{1}{q} = 1$,

$$ab \leq \frac{c^p}{p} a^p + \frac{c^{-q}}{q} b^q,$$

and equality holds if and only if $a^p = b^q$.

Theorem: Considering the system (2) with observer (3) and adaptive law (4) then $\hat{x}_1 \rightarrow x_1, \hat{x}_2 \rightarrow x_2, \hat{x}_3 \rightarrow \phi$

Proof: Following (Khalil & Praly, 2014), because the f is a known function of $f(x_1, x_2, u)$, we can take $\hat{f} = f$ where \hat{f} is the estimation of f . From (2) and (3), we have the error dynamics

$$\begin{cases} \dot{e}_1 = -\kappa_1 |e_1|^{\frac{2}{3}} \text{sgn}(e_1) + e_2 \\ \dot{e}_2 = -\kappa_2 |e_1|^{\frac{1}{3}} \text{sgn}(e_1) + e_3 \\ \dot{e}_3 = -\kappa_3 \text{sgn}(e_1) \end{cases} \quad (5)$$

where $e_3 = \phi(x_1, x_2, t) - \hat{x}_3$. Let $z_1 = \frac{e_1}{1}; z_2 = \frac{e_2}{\kappa_1}; z_3 = \frac{e_3}{\kappa_2}$ then (5) become as

$$\begin{cases} \dot{z}_1 = -k_1 \left(|z_1|^{\frac{2}{3}} \text{sgn}(z_1) - z_2 \right) \\ \dot{z}_2 = -k_2 \left(|z_1|^{\frac{1}{3}} \text{sgn}(z_1) - z_3 \right) \\ \dot{z}_3 = -k_3 \text{sgn}(z_1) \end{cases} \quad (6)$$

where $k_1 = \kappa_1, k_2 = \frac{\kappa_2}{\kappa_1}, k_3 = \frac{\kappa_3}{\kappa_2}$

(6) can be rewritten as

$$\begin{cases} \dot{z}_1 = -k_1 \left([z_1]^{\frac{2}{3}} - z_2 \right) \\ \dot{z}_2 = -k_2 \left([z_1]^{\frac{1}{3}} - z_3 \right) \\ \dot{z}_3 = -k_3 [z_1]^0 \end{cases} \quad (7)$$

where $[z_k]^n = |z_k|^n \text{sgn}(z_k)$, $z_k = [z_k]^1 = |z_k| \text{sgn}(z_k)$ and $[z_k]^0 = \text{sgn}(z_k)$ ($n, k \in \mathfrak{N}$)

Let's define the Lyapunov function as

$$V = V_1 + V_2 \quad (8)$$

where

$$V_1(z) = Z_1(z_1, z_2) + \beta_1 Z_2(z_2, z_3) + \beta_2 \frac{1}{5} |z_3|^5 \quad (9)$$

which β_1 , and β_2 are positive.

$$\begin{cases} Z_1(z_1, z_2) = \frac{3}{5} |z_1|^{\frac{5}{3}} - z_1 z_2 + \frac{2}{5} |z_2|^{\frac{5}{2}} \\ Z_2(z_2, z_3) = \frac{2}{5} |z_2|^{\frac{5}{2}} - z_2 [z_3]^3 + \frac{3}{5} |z_3|^5 \end{cases} \quad (10)$$

Using Lemma 3.2 for $z_1 z_2$ and $z_2 [z_3]^3$ term, we have

$$\begin{cases} z_1 z_2 \leq \frac{3}{5} |z_1|^{\frac{5}{3}} + \frac{2}{5} |z_2|^{\frac{5}{2}} \\ z_2 [z_3]^3 \leq \frac{2}{5} |z_2|^{\frac{5}{2}} + \frac{3}{5} |z_3|^5 \end{cases} \quad (11)$$

Therefore,

$$\begin{cases} Z_1(z_1, z_2) \geq 0 \\ Z_2(z_2, z_3) \geq 0 \end{cases} \quad (12)$$

From (9) and (12), we have $V_1 \geq 0$ and

$$V_2 = \frac{1}{2\Lambda} (L - L^*)^2 \geq 0 \quad (13)$$

where L^* are positive constants.

From derivative (8), we have

$$\dot{V} = \dot{V}_1 + \dot{V}_2 \quad (14)$$

Let's consider \dot{V}_1

$$\begin{aligned} \dot{V}_1 &= \sigma_1 \dot{z}_1 - |z_2|^0 \lambda_1 \dot{z}_2 + \beta_1 \sigma_2 \dot{z}_2 \\ &\quad - 3\beta_1 |z_3|^2 \lambda_2 \dot{z}_3 + \beta_2 [z_3]^4 \dot{z}_3 \end{aligned} \quad (15)$$

where $\sigma_1 = [z_1]^{\frac{2}{3}} - z_2$, $\sigma_2 = [z_2]^{\frac{3}{2}} - [z_3]^3$, $\lambda_1 = z_1 - [z_2]^{\frac{3}{2}}$ and $\lambda_2 = z_2 - [z_3]^2$. We can rewrite (15) as

$$\dot{V}_1 = -W_1(z) \quad (16)$$

where

$$\begin{aligned} W_1(z) &= -\sigma_1 \dot{z}_1 + |z_2|^0 \lambda_1 \dot{z}_2 - \beta_1 \sigma_2 \dot{z}_2 \\ &\quad + 3\beta_1 |z_3|^2 \lambda_2 \dot{z}_3 - \beta_2 [z_3]^4 \dot{z}_3 \end{aligned} \quad (17)$$

By substituting (7) into (17), we have

$$\begin{aligned} W_1(z) &= k_1 \underbrace{\left([z_1]^{\frac{2}{3}} - z_2 \right) \left([z_1]^{\frac{2}{3}} - z_2 \right)}_{\eta_1} \\ &\quad - |z_2|^0 k_2 \left([z_1]^{\frac{1}{3}} - z_3 \right) \left(z_1 - [z_2]^{\frac{3}{2}} \right) \\ &\quad + k_2 \beta_1 \left([z_2]^{\frac{3}{2}} - [z_3]^3 \right) \left([z_1]^{\frac{1}{3}} - z_3 \right) \\ &\quad - 3\beta_1 k_3 [z_1]^0 |z_3|^2 (z_2 - [z_3]^2) \\ &\quad + \beta_2 k_3 [z_1]^0 [z_3]^4 \\ &= k_1 \eta_1(z_1, z_2) + \mu_1(z) \end{aligned} \quad (18)$$

In (18) η_1 is non-negative, and it vanishes when $[z_1]^{\frac{2}{3}} = z_2$. According to Lemma 3.1 there exists a sufficiently large positive value of k_1 such as $W_1(z) > 0$ if the value of μ_1 restricted to $[z_1]^{\frac{2}{3}} = z_2$ is positive. From (18), it is seen that $W_2(z)$ can be written as

$$\begin{aligned} W_2(z) &= k_2 \beta_1 \left([z_2]^{\frac{3}{2}} - [z_3]^3 \right) \left([z_1]^{\frac{1}{3}} - z_3 \right) \\ &\quad - 3\beta_1 k_3 [z_1]^0 |z_3|^2 (z_2 - [z_3]^2) \\ &\quad + \beta_2 k_3 [z_1]^0 [z_3]^4 \\ &= k_2 \beta_1 \left([z_2]^{\frac{3}{2}} - [z_3]^3 \right) \left([z_2]^{\frac{1}{2}} - z_3 \right) \\ &\quad - 3\beta_1 k_3 [z_1]^0 |z_3|^2 (z_2 - [z_3]^2) \\ &\quad + \beta_2 k_3 [z_1]^0 [z_3]^4 \\ &= k_2 \eta_2 + \mu_2(z) \end{aligned} \quad (19)$$

In (19) η_2 is positive on and it vanishes when $[z_2]^{\frac{1}{2}} = z_3$. In Lemma 3.1, there is a sufficiently large positive value of k_2 such that $W_2(z)$ is positive definite on $[z_2]^{\frac{1}{2}} = z_3$ if $\mu_2(z)$ is positive. From (21) we see that $\mu_2 = k_3 \beta_2 [z_2]^0 [z_3]^4 = k_3 \beta_2 |z_3|^4$ is positive on $[z_2]^{\frac{1}{2}} = z_3$. We conclude that $W_2(z) \geq 0$. Therefore, $\dot{V}_1 \leq 0$.

Let's consider \dot{V}_2

$$\dot{V}_2 = \frac{1}{\Lambda} (L - L^*) \dot{L} \quad (20)$$

By substituting (4) into (20), we have

$$\dot{V}_2 = \frac{1}{\Lambda} (L - L^*) \bar{L} |e_1| \text{sign}(|e_1| - \varepsilon) \quad (21)$$

By substituting (21) and (16) into (14), we have

$$\begin{aligned} \dot{V} &= -W_1(z) + \frac{1}{\Lambda} (L - L^*) \bar{L} |e_1| \text{sign}(|e_1| - \varepsilon) \\ &\leq -W_1(z) + \underbrace{\frac{1}{\Lambda} |L - L^*| \bar{L} |e_1| \text{sign}(|e_1| - \varepsilon)}_{\zeta} \end{aligned} \quad (22)$$

Case 1: $|e_1| < \varepsilon$. In this case $\zeta \leq 0$ so that $\dot{V} \leq -W_1(z)$

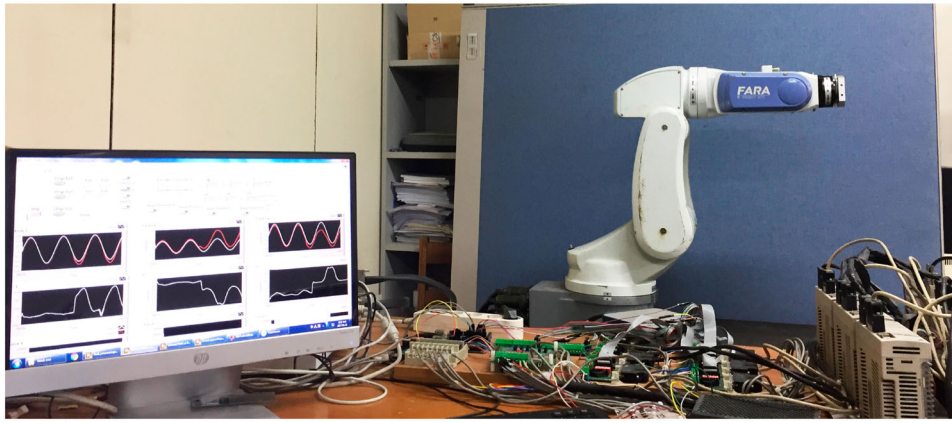


Figure 2. Real-system 3-DOF robot manipulator.

Case 2: $|e_1| \geq \varepsilon$. In this case $\zeta \geq 0$ so that (20) can be positive, it can not conclude system stability. Therefore, $|e_1|$ can be decreased. As soon as $|e_1|$ less than ε and the system returns to the previous case. The theorem is proved. ■

4. Experimental results

4.1. Hardware set-up

The experimental set-up is shown in Figure 2 with a 3-DOF FARA-AT2 robot manipulator. This robot manipulator has 6-DOF, but for these experiments, joints 4-5-6 are blocked. The 3-DOF FARA-AT2 robot has a CSMP series motor at each joint. The CSMP-02BB driver is used for joints 1 and 2, while the CSMP-01BB driver is used for joint 3. The gear box at each joint is 120:1, 120:1, 100:1 at joints 1, 2 and 3, respectively. The encoder at each joint is an incremental encoder with 2048 lines. The controller runs on Labview-FPGA NI-PXI-8110 and NI-PXI-7842R PXI cards with frequency control set at 500 Hz. NI-PXI-8110 runs on a Windows operating system. The low-level controller is PD applied to 3 joints of the robot manipulator where $K_D = \text{diag}(150, 140, 140)$ and $K_p = \text{diag}(800, 2500, 2500)$ were selected.

4.2. Contact detection

In this section, we present the results of contact detection between humans and robots. Safety is one of the fundamentals of pHRI. Therefore, detection of the whole body of the robot is necessary and enjoys much attention in numerous research studies in pHRI using different methods. In this experiment, the robot pauses every time a contact is detected and resumes tracking its trajectory after 3 s. The threshold technique is used to detect the contact force and false alarm. For simplicity, in this experiment, the threshold value is set at each joint.

Desired tracking trajectory of the end-effector:

$$\begin{cases} x_d = 0 \\ y_d = 0.15 \sin\left(\frac{\pi t}{1600}\right) \\ z_d = 0.15 \sin\left(\frac{\pi t}{1600}\right) - 0.15 \end{cases} \quad (23)$$

In Figure 3, the collision detection is shown. The collision occurs at $t = 11, 17, 23, 29, 39.5, 48$ s. It can be detected in the whole-body robot. In Figure 4, the joint positions are shown in case collision. Figure 4 shows the position trajectory of the desired trajectory remained. The stop within 3 s of the robot only delays time so that the robot still can complete the task. This scenario is usually used in Level 3 of a collaborative robot. The snapshot of the touching robot with the position of touching is shown in Figure 5.

4.3. Human push/pull

In this section, the interaction between humans and robots is based on admittance control.

$$\frac{x'_d(s)}{\Gamma(s)} = \frac{1}{Ms^2 + Bs + K} \quad (24)$$

where s is the complex argument. $x'_d(s)$ is the desired reference for the inner loop control. $\Gamma(s)$ is the external force/torque vector applied by the operator. $Z(s) = Ms^2 + Bs + K$ represents the environmental impedance where $M, B, K \in R^{n \times n}$ denote the mass, damping, and stiffness of the admittance model.

The human pushes/pulls the robot at different points and different links. The block diagram of admittance control uses an adaptive third-order sliding mode observer, is shown in Figure 6. The estimated contact force during the physical human-robot interaction is shown in Figure 7.

Figure 7 shows that contact force estimation can be used for admittance control in physical human-robot

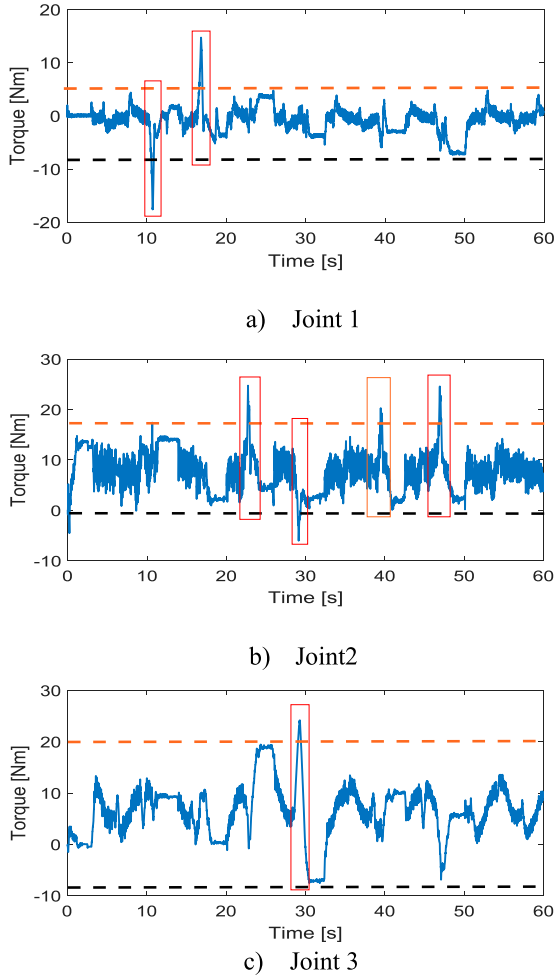


Figure 3. Detection of contact force. (a) Joint 1. (b) Joint 2. (c) Joint 3.

interaction. The human can interact with the whole body of a robot. The accuracy of the interaction force estimation depends on the accuracy of the dynamic model of the robot manipulator. Therefore, the identification process is of great importance in the estimation of the contact force based on a model. The snapshots of push and pull are shown in Figure 8. In addition, the tracking trajectory at joints is shown in Figure 9.



Figure 5. Snapshot of the touching robot experiment.

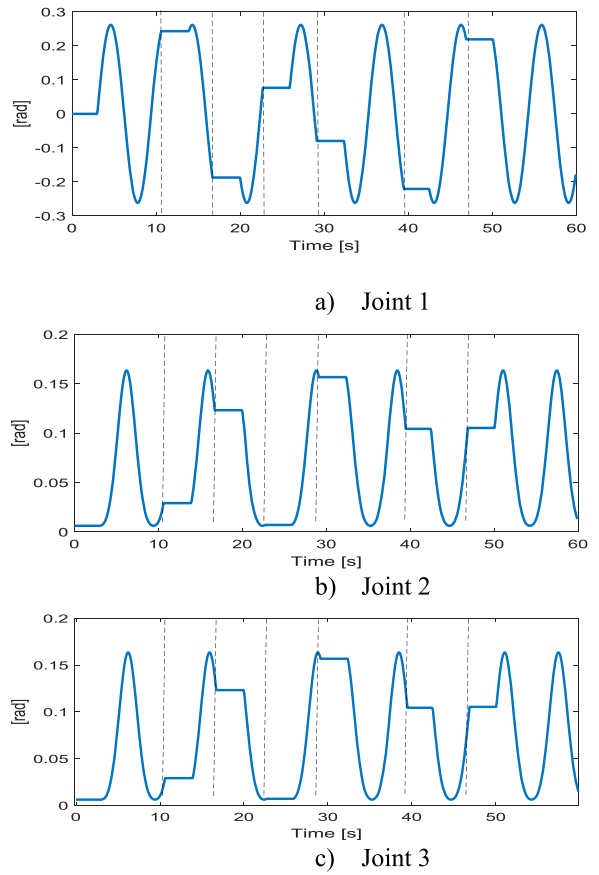


Figure 4. Tracking trajectory of joints. (a) Joint 1. (b) Joint 2. (c) Joint 3.

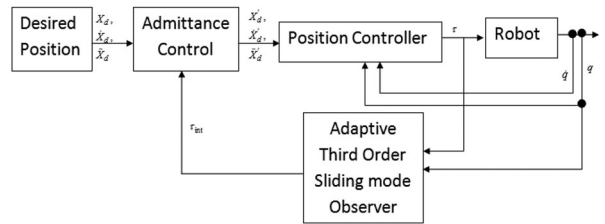


Figure 6. Admittance control.

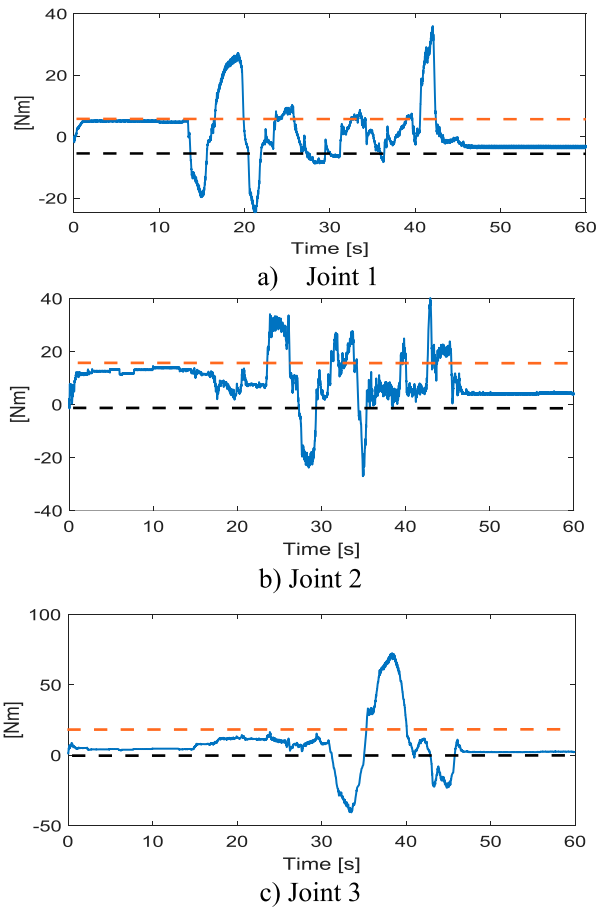


Figure 7. Contact Force estimation. (a) Joint 1. (b) Joint 2. (c) Joint 3.

Remark: The threshold value in this paper was chosen based on the experience. The value of thresholds highly depends on the accuracy of the dynamic model of the robot. When the dynamic parameters of the robot have high accuracy, the threshold value is small and close to zero. The threshold value can be specified for the bounded internal dynamic uncertainties of the robot. Therefore, in the theorem, this value does not change too much when the robot moves or stops. However, in practice, due to the low accuracy of the robot's dynamic parameters, the selection of threshold is highly based on

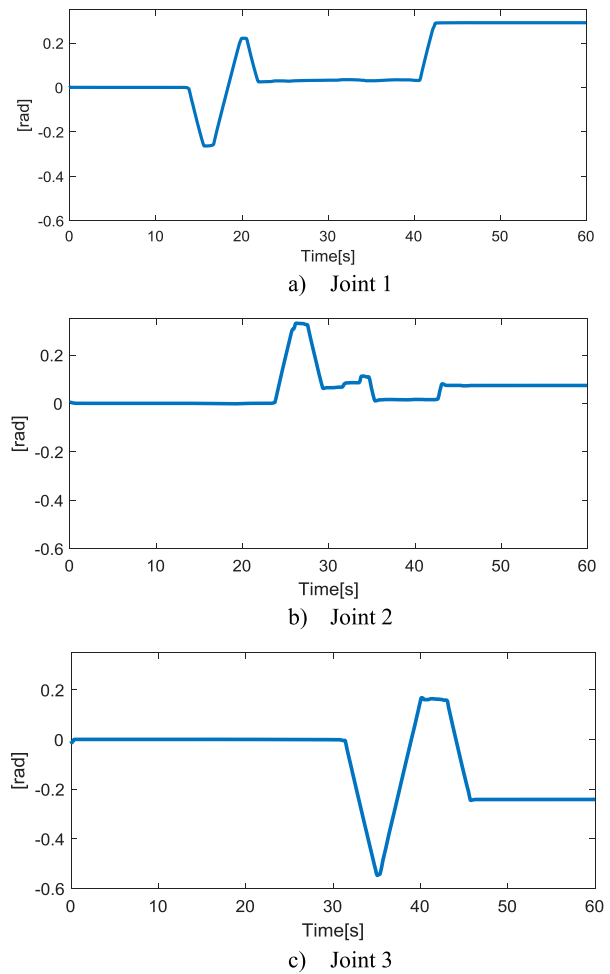


Figure 9. Tracking trajectory of joints. (a) Joint 1. (b) Joint 2. (c) Joint 3.

the operator's experience. This threshold value will be effective in the detection of torque value. In this work, the value of torque can be detected quite high due to the low accuracy of the robot's dynamic parameters in the identification step. In the future, with the improvement of identification step, the range of torque detection can be wider meaning that the threshold value should be close to zero.



Figure 8. Snapshot of push and Pull robot experiment.

5. Conclusion

In this paper, the estimation of contact force using the adaptive third-order sliding mode observer was proposed to assess the interaction of contact force. Experimental results in two scenarios, detection contact and push/pull, illustrate the effectiveness of the approach method in collaborative robots. However, the accuracy of this method is highly dependent on the accuracy of the identification step in the model dynamics. To overcome this problem, the threshold is used to detect the contact and estimate the contact force to use this information for admittance control. In future research, the optimization and intelligent technique (Han & Huang, 2006; Huang et al., 2005; Huang & Jiang, 2012; Sun, Huang, and Fang, 2005; Sun, Huang, Fang, and Yang, 2005; Xu & Huang, 2008; Zhao et al., 2004) is used to optimize the observer parameter and improve the performance.

Disclosure statement

No potential conflict of interest was reported by the author(s).

Funding

This research was supported by Basic Science Research Program through the National Research Foundation of Korea (NRF) funded by the Ministry of Education (NRF-2016R1D1A3B0393 0496).

References

- Bahrami, M., Naraghi, M., & Zareinejad, M. (2018). Adaptive super-twisting observer for fault reconstruction in electro-hydraulic systems. *ISA Transactions*, 76, 235–245. <https://doi.org/10.1016/j.isatra.2018.03.014>
- Bauer, W., Bender, M., Braun, M., Rally, P., & Scholtz, O. (2016). *Lightweight robots in manual assembly—best to start simply*. Fraunhofer-Institut für Arbeitswirtschaft und organ. IAO.
- Chen, S., Luo, M., & He, F. (2018). A universal algorithm for sensorless collision detection of robot actuator faults. *Advances in Mechanical Engineering*, 10(1), <https://doi.org/10.1177/1687814017740710>.
- Chen, W.-S., Yuen, P. C., Huang, J., & Dai, D.-Q. (2005). Kernel machine-based one-parameter regularized fisher discriminant method for face recognition. *IEEE Transactions on Systems, Man and Cybernetics, Part B (Cybernetics)*, 35(4), 659–669. <https://doi.org/10.1109/TSMCB.2005.844596>
- Cirillo, A., Ficuciello, F., Natale, C., Pirozzi, S., & Villani, L. (2016). A conformable force/tactile skin for physical human–robot interaction. *IEEE Robotics and Automation Letters*, 1(1), 41–48. <https://doi.org/10.1109/LRA.2015.2505061>
- Cruz-Zavala, E., & Moreno, J. A. (2016). Lyapunov functions for continuous and discontinuous differentiators. *IFAC-Papers OnLine*, 49(18), 660–665. <https://doi.org/10.1016/j.ifacol.2016.10.241>
- Dao, P. N., Do, D. K., & Nguyen, D. K. (2021). Adaptive Reinforcement learning-enhanced motion/force control strategy for multirobot systems. *Mathematical Problems in Engineering*, 2021(18). <https://doi.org/10.1155/2021/5560277>
- De Luca, A., & Mattone, R. (2005). *Sensorless robot collision detection and hybrid force/motion control*. In Proceedings of the 2005 IEEE International Conference on Robotics and Automation, 2005. ICRA 2005, 12–17 May 2009, pp. 999–1004.
- Du, J.-X., Huang, D.-S., Wang, X.-F., & Gu, X. (2007). Shape recognition based on neural networks trained by differential evolution algorithm. *Neurocomputing*, 70(4–6), 896–903. <https://doi.org/10.1016/j.neucom.2006.10.026>
- Du, J.-X., Huang, D.-S., Zhang, G.-J., & Wang, Z.-F. (2006). A novel full structure optimization algorithm for radial basis probabilistic neural networks. *Neurocomputing*, 70(1–3), 592–596. <https://doi.org/10.1016/j.neucom.2006.05.003>
- Duchaine, V., Lauzier, N., Baril, M., Lacasse, M.-A., & Gosselin, C. (2009). *A flexible robot skin for safe physical human robot interaction*. In: IEEE International Conference on Robotics and Automation, 2009. ICRA'09, 12–17 May 2009, pp. 3676–3681.
- Ebert, D., & Henrich, D. (2002). Safe human-robot-cooperation: Image-based collision detection for industrial robots. IEEE/RSJ International Conference on Intelligent Robots and Systems 2002. Date of Conference: 30 September–4 October 2002. Lausanne, Switzerland
- Eom, K. S., Suh, I. H., Chung, W. K., & Oh, S.-R. (1998). *Disturbance observer based force control of robot manipulator without force sensor*. In: Proceedings. 1998 IEEE International Conference on Robotics and Automation, 1998, 20–20 May 1998. pp. 3012–3017.
- Ferretti, G., Magnani, G., & Rocco, P. (1997). Toward the implementation of hybrid position/force control in industrial robots. *IEEE Transactions on Robotics and Automation*, 13(6), 838–845. <https://doi.org/10.1109/70.650162>
- Fridman, L., Shtessel, Y., Edwards, C., & Yan, X.-G. (2008). Higher-order sliding-mode observer for state estimation and input reconstruction in nonlinear systems. *International Journal of Robust and Nonlinear Control*, 18(4–5), 399–412. <https://doi.org/10.1002/rnc.1198>
- Gaz, C., Magrini, E., & De Luca, A. (2018). A model-based residual approach for human-robot collaboration during manual polishing operations. *Mechatronics*, 22(2018), 234–247. <https://doi.org/10.1016/j.mechatronics.2018.02.014>
- Geravand, M., Flacco, F., & De Luca, A. (2013). *Human-robot physical interaction and collaboration using an industrial robot with a closed control architecture*. In 2013 IEEE International Conference on Robotics and Automation, pp. 4000–4007. <https://doi.org/10.1109/ICRA.2013.6631141>
- Han, F., & Huang, D.-S. (2006). Improved extreme learning machine for function approximation by encoding a priori information. *Neurocomputing*, 69(16–18), 2369–2373. <https://doi.org/10.1016/j.neucom.2006.02.013>
- Han, F., & Huang, D.-S. (2008). A new constrained learning algorithm for function approximation by encoding a priori information into feedforward neural networks. *Neural Computing and Applications*, 17(5–6), 433–439. <https://doi.org/10.1007/s00521-007-0135-5>
- Han, F., Ling, Q.-H., & Huang, D.-S. (2008). Modified constrained learning algorithms incorporating additional functional constraints into neural networks. *Information Sciences*, 178(3), 907–919. <https://doi.org/10.1016/j.ins.2007.09.008>
- Han, F., Ling, Q.-H., & Huang, D.-S. (2010). An improved approximation approach incorporating particle swarm optimization

- and a priori information into neural networks. *Neural Computing and Applications*, 19(2), 255–261. <https://doi.org/10.1007/s00521-009-0274-y>
- Hogan, N. (1984). *Impedance control: An approach to manipulation*. In American Control Conference, 1984, 6–8 June 1984. pp. 304–313.
- Hu, J., & Xiong, R. (2018). Contact force estimation for robot manipulator using semiparametric model and disturbance Kalman Filter. *IEEE Transactions on Industrial Electronics*, 65(4), 3365–3375. <https://doi.org/10.1109/TIE.2017.2748056>
- Huang, D. (1999). Radial basis probabilistic neural networks: Model and application. *International Journal of Pattern Recognition and Artificial Intelligence*, 13(07), 1083–1101. <https://doi.org/10.1142/S0218001499000604>
- Huang, D.-S., & Du, J.-X. (2008). A constructive hybrid structure optimization methodology for radial basis probabilistic neural networks. *IEEE Transactions on Neural Networks*, 19(12), 2099–2115. <https://doi.org/10.1109/TNN.2008.2004370>
- Huang, D.-S., & Jiang, W. (2012). A general CPL-AdS methodology for fixing dynamic parameters in dual environments. *IEEE Transactions on Systems, Man, and Cybernetics, Part B (Cybernetics)*, 42(5), 1489–1500. <https://doi.org/10.1109/TSMCB.2012.2192475>
- Huang, G.-B., Mao, K. Z., Siew, C.-K., & Huang, D.-S. (2005). Fast modular network implementation for support vector machines. *IEEE Transactions on Neural Networks*, 16(6), 1651–1663. <https://doi.org/10.1109/TNN.2005.857952>
- Jung, S., Hsia, T. C., & Bonitz, R. G. (2004). Force tracking impedance control of robot manipulators under unknown environment. *IEEE Transactions on Control Systems Technology*, 12(3), 474–483. <https://doi.org/10.1109/TCST.2004.824320>
- Khalil, H. K. (2017). Cascade high-gain observers in output feedback control. *Automatica*, 80, 110–118. <https://doi.org/10.1016/j.automatica.2017.02.031>
- Khalil, H. K., & Praly, L. (2014). High-gain observers in nonlinear feedback control. *International Journal of Robust and Nonlinear Control*, 24(6), 993–1015. <https://doi.org/10.1002/rnc.3051>
- Kommuri, S. K., Rath, J. J., & Veluvolu, K. C. (2018). Sliding-Mode-Based observer–controller structure for fault-resilient control in DC servomotors. *IEEE Transactions on Industrial Electronics*, 65(1), 918–929. <https://doi.org/10.1109/TIE.2017.2721883>
- Le, Q. D., & Kang, H.-J. (2020). Implementation of fault-tolerant control for a robot manipulator based on synchronous sliding mode control. *Applied Sciences*, 10(7), 2534. <https://doi.org/10.3390/app10072534>
- Le, Q. D., & Kang, H.-J. (2021). Sensor-Less contact force estimation in physical human-robot interaction. In D.-S. Huang, K.-H. Jo, J. Li, V. Gribova, & A. Hussain (Eds.), *Intelligent computing theories and application* (pp. 233–244). Springer International Publishing.
- Luo, D., Xiong, X., Jin, S., & Kamal, S. (2018). Adaptive gains of dual level to super-twisting algorithm for sliding mode design. *IET Control Theory & Applications*, 12(17), 2347–2356. <https://doi.org/10.1049/iet-cta.2018.5380>
- Magrini, E., Flacco, F., & De Luca, A. (2014). *Estimation of contact forces using a virtual force sensor*. In: 2014 IEEE/RSJ International Conference on Intelligent Robots and Systems (IROS 2014), 14–18 September 2014, pp. 2126–2133.
- Magrini, E., Flacco, F., & De Luca, A. (2015). *Control of generalized contact motion and force in physical human-robot interaction*. In 2015 IEEE International Conference on Robotics and Automation (ICRA), 26–30 May 2015, pp. 2298–2304.
- Mörtl, A., Lawitzky, M., Kucukyilmaz, A., Sezgin, M., Basdogan, C., & Hirche, S. (2012). The role of roles: Physical cooperation between humans and robots. *The International Journal of Robotics Research*, 31(13), 1656–1674. <https://doi.org/10.1177/0278364912455366>
- Ortiz-Ricardez, F. A., Sánchez, T., & Moreno, J. A. (2015). *Smooth Lyapunov function and gain design for a second order differentiator*. In 2015 IEEE 54th Annual Conference on Decision and Control (CDC), 15–18 December 2015, pp. 5402–5407.
- Peshkin, M. A., Colgate, J. E., Wannasupphoprasit, W., Moore, C. A., Gillespie, R. B., & Akella, P. (2001). Cobot architecture. *IEEE Transactions on Robotics and Automation*, 17(4), 377–390. <https://doi.org/10.1109/70.954751>
- Stolt, A., Robertsson, A., & Johansson, R. (2015). *Robotic force estimation using dithering to decrease the low velocity friction uncertainties*. In 2015 IEEE International Conference on Robotics and Automation (ICRA), 26–30 May 2015, pp. 3896–3902.
- Suita, K., Yamada, Y., Tsuchida, N., Imai, K., Ikeda, H., & Sugimoto, N. (1995). *A failure-to-safety “Kyozon” system with simple contact detection and stop capabilities for safe human-autonomous robot coexistence*. In Proceedings, 1995 IEEE International Conference on Robotics and Automation, 21–27 May 1995, pp. 3089–3096.
- Sun, B.-Y., Huang, D.-S., & Fang, H.-T. (2005). Lidar signal denoising using least-squares support vector machine. *IEEE Signal Processing Letters*, 12(2), 101–104. <https://doi.org/10.1109/LSP.2004.836938>
- Sun, B.-Y., Huang, D.-S., Fang, H.-T., & Yang, X.-M. (2005). A novel robust regression approach of lidar signal based on modified least squares support vector machine. *International Journal of Pattern Recognition and Artificial Intelligence*, 19(05), 715–729. <https://doi.org/10.1142/S021800140500423X>
- Van, M., Ge, S. S., & Ren, H. (2017). Robust fault-tolerant control for a class of second-order nonlinear systems using an adaptive third-order sliding mode control. *IEEE Transactions on Systems, Man, and Cybernetics: Systems*, 47(2), 221–228. <https://doi.org/10.1109/TSMC.2016.2557220>
- Wahrburg, A., Bös, J., Listmann, K. D., Dai, F., Matthias, B., & Ding, H. (2017). Motor-current-based estimation of cartesian contact forces and torques for robotic manipulators and its application to force control. *IEEE Transactions on Automation Science and Engineering*, 15(2), 879–886. <https://doi.org/10.1109/TASE.2017.2691136>
- Wang, X.-F., & Huang, D.-S. (2009). A novel density-based clustering framework by using level set method. *IEEE Transactions on Knowledge and Data Engineering*, 21(11), 1515–1531. <https://doi.org/10.1109/TKDE.2009.21>
- Wang, X.-F., Huang, D.-S., & Xu, H. (2010). An efficient local Chan–Vese model for image segmentation. *Pattern Recognition*, 43(3), 603–618. <https://doi.org/10.1016/j.patcog.2009.08.002>
- Wojtara, T., Uchihara, M., Murayama, H., Shimoda, S., Sakai, S., Fujimoto, H., & Kimura, H. (2009). Human–robot collaboration in precise positioning of a three-dimensional object. *Automatica*, 45(2), 333–342. <https://doi.org/10.1016/j.automatica.2008.08.021>

Xu, H., & Huang, D.-S. (2008). *One class support vector machines for distinguishing photographs and graphics*. In 2008 IEEE International Conference on Networking, Sensing and Control, 6–8 April 2008, pp. 602–607.

Yu, W., & Perrusquia, A. (2022). Reinforcement learning for robot position/force control. In *Human-robot interaction*

control using reinforcement learning (pp. 97–118). IEEE.

Zhao, Z.-Q., Huang, D.-S., & Sun, B.-Y. (2004). Human face recognition based on multi-features using neural networks committee. *Pattern Recognition Letters*, 25(12), 1351–1358. <https://doi.org/10.1016/j.patrec.2004.05.008>